Fracture Mechanics of Concrete and Concrete Structures - Recent Advances in Fracture Mechanics of Concrete - B. H. Oh, et al.(eds)
ⓒ 2010 Korea Concrete Institute, Seoul, ISBN 978-89-5708-180-8

Misconceptions on Variability of Fracture Energy, Its Uniaxial Definition by Work of Fracture, and Its Presumed Dependence on Crack Length and Specimen Size

Z. P. Bažant[1], Qiang Yu[1], Gianluca Cusatis[2], Luigi Cedolin[3], Milan Jirásek[4]
[1]*Northwestern University, Department of Civil and Environmental Engineering, Illinois 60208, USA.*
[2]*Rensselaer Polytechnic Institute, Troy, New York, USA.*
[3]*Politecnico di Milano, Milan, Italy.*
[4]*Czech Technical University, Prague.*

ABSTRACT: Recent polemics on fracture testing of concrete and mathematical modeling of the size effect impede the efforts to introduce of fracture mechanics into the design practice, and especially into the design codes. To overcome this barrier to progress, this paper compares the Hu-Duan Boundary Effect Model (BEM) promulgated during the last decade to the Size-Shape Effect Law (SEL) proposed at Northwestern University in 1984 and extended to the geometry (or shape) effects in 1990. The comparison shows that within a rather limited part of the range of sizes and shapes, the fracture energy values identified by BEM and SEL from maximum load data are nearly the same. But in other parts of the range the BEM is found to be either inferior or inapplicable. Several hypotheses of BEM are shown to be unrealistic. The material tensile strength values identified by BEM are found to be inconsistent with the cohesive crack model and have a much larger error than those obtained from the SEL. As a related problem, it is shown that without testing at various specimen sizes, the cohesive softening stress-separation law determined from the work-of-fracture method or from the two-parameter model is non-unique. Especially, the same data can be fitted with very different values of the initial fracture energy (area under the initial tangent) and of the tensile strength limit, which give very different size and shape effects on the nominal strength of structure. Finally it must be emphasized that formulation of a coherent fracture theory for a quasibrittle material such a concrete is impossible without capturing the size effect.

1 INTRODUCTION

Interpreting various experimental observations, some investigators recently suggest that the fracture energy, G_F, of concrete is not a constant, but varies with the crack length and structure size. There are two objections to such an interpretation: 1) It destroys the theory unless some rule for the variation of G_F, involving another fundamental constant, is introduced; and 2) it relies on a uniaxial definition of G_F as the work of the cohesive stress on the crack face separation at a fixed point, whereas the correct definition of G_F must be based on the J-integral, i.e., on the flux of energy into the fracture process zone propagating in a stationary way.

The condition of stationary propagation requires that the boundaries be sufficiently remote compared to the size of the fracture process zone and material inhomogeneities. This condition is always satisfied for normal-scale specimens of fine grained ceramics and metals, but not for concrete, for which the comparable specimen size would be prohibitively large (the maximum aggregate size times at least 10^2, possibly 10^3).

Therefore, G_F must be defined either by extrapolation to infinite structure size, or by fitting of the test data by a theory that automatically exhibits the size effect, e.g. by the nonlocal softening damage model, by the random lattice particle model or, in a simpler but more limited way, by the cohesive crack model. These models can explain the observations of apparent variation of fracture energy by a reduction of the fracture process zone size in areas adjacent to the body surface. In the case of no initial crack or notch, full explanation of such observations further requires taking into account the Weibull statistical size effect.

Further it must be noted that G_F cannot be measured by uniaxial tensile tests assuming the crack face separation to be uniform across the specimen width, that the testing of the work-of-fracture cannot capture the tail of the softening curve, and that the G_F values estimated from the measured work of fracture have a very high statistical scatter.

For this reason, it is preferable to focus fracture testing on the initial fracture energy G_f (area under the initial slope of the cohesive softening curve). G_f can be identified from size effect tests of typical laboratory specimens, is by definition size-independent, and has a much smaller coefficient of variation than G_F.

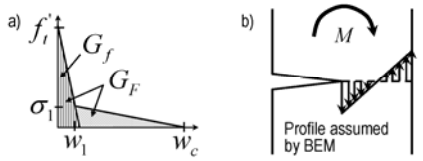

Fig. 1: a) Bilinear softening curve and its key parameters of cohesive crack model; b) linear stress profile assumed in BEM.

It is well established that concrete, an archetypical quasibrittle material, exhibits a transitional deterministic (energetic) size effect if a deep notch or a large traction-free crack exists (Bažant 1984). This is now called the Type 2 size effect. A different deterministic size effect, now called Type 1, was also identified in concrete structures with no notch (Bažant and Li 1995). Both size effects are automatically exhibited by the cohesive crack model and crack band model. The former was proposed by Barenblatt (1959), finalized by Rice (1968) (who proved the equality of work of fracture to the energy flux into the fracture front), and pioneered for concrete by Hillerborg et al. (1976), Petersson (1981) and Hillerborg (1985) under the alternative name "fictitious crack model".

A bilinear softening curve has been widely adopted for a realistic and simple description of the relation of cohesive stress and the crack face separation. Its two key parameters are the total fracture energy G_F and initial fracture energy G_f. G_F is defined as the energy (per unit area) required for complete break, and represents the total area under the softening curve (Fig. 1a). The initial fracture energy G_f is defined as the area under the initial tangent of the bilinear softening curve; see Fig. 1a.

According to its definition, the most straightforward way to identify G_F is the work-of-fracture method. Ideally, G_F is obtained as the area under the measured complete load-deflection curve in which a notched specimen is totally broken, divided by the total crack area (or ligament area). As simple as the concept seems, it nevertheless yields problematic results. It is found that the fracture energy G_F of concrete measured by the work-of-fracture method is not a constant. Instead, it is also size dependent (Nallathambi et al. 1984, Wittmann et al. 1990, Hu and Wittmann 1992). Contrary to the nominal strength, the measured fracture energy increases with an increasing size. From the trend shown in the measured fracture energy versus size plot, it can be extrapolated that the measured fracture energy will reach a horizontal asymptote as size is large enough.

One recent model that attempts to explain the observations is the boundary effect model (BEM) of Hu and Duan (Hu and Duan 2007, 2008, 2009). Here, a recent critical analysis of this model (Yu et al. 2010) and its comparison with the size-shape effect law (SEL), with experiments and with the cohesive crack model will be summarized. Hopefully, this would yield a better understanding of the nature of the size effect and fracture energy, and thus lead to a better description of concrete fracture.

2 SIZE-SHAPE EFFECT LAW (SEL) AND BOUNDARY EFFECT MODEL (BEM)

The size effect law (SEL), also called the size-shape effect law because the geometry effects were included in its 1990 generalization (Bažant and Kazemi 1990), considers the deterministic size effect in concrete and other quasibrittle materials to be caused by the energy release due to stress redistribution by fracture growth. The SEL is of two basic types.

Type 2. It applies to structures with a deep notch or large traction-free crack. It can be written as (Bažant 1984, 1997, 2004, 2005):

$$\sigma_N = P/bD = \hat{B} f_t'(1 + D/D_0)^{-1/2} \quad (1)$$

$$D_0 = c_f g'(\alpha_0)/g(\alpha_0), \quad \hat{B} f_t' = \sqrt{EG_f / g'(\alpha_0) c_f} \quad (2)$$

here P = peak load, D = characteristic size of a two-dimensionally similar structure, b = width of structure, f'_t = tensile strength, E = Young's elastic modulus; $\alpha_0 = a_0 / D$ = initial crack- or notch-to-depth ratio; $g(\alpha)$ = dimensionless energy release function of linear elastic fracture mechanics (LEFM), which introduces the geometry effects; G_f = initial fracture energy; and c_f = material length constant representing the distance from crack tip to the resultant of tensile strength in the fracture process zone (FPZ).

Type 1. It applies to structures of positive geometry (i.e. $g'(\alpha) > 0$) failing at crack initiation from a smooth surface. It reads (Bažant and Li 1995, Bažant 2005):

$$\sigma_N = \sigma_\infty (1 + rD_b / D)^{1/r} \quad (3)$$

where $D_b = \left\langle -g''(0) c_f / 4g'(0) \right\rangle$, $\sigma_\infty = [EG_f / c_f g'_0]^{1/2}$, $\left\langle x \right\rangle = \max(x, 0)$, and r = empirical parameter. σ_∞ is a constant representing the large size asymptote, and $D_b \approx$ double the thickness of the boundary layer of cracking in beam flexure. According to Eq. (3), the size effect will vanish for large sizes because the boundary layer is negligible compared to the size D. Due to the material randomness, the Weibull's statistical size effect, which is much weaker than the deterministic size effect, must dominate for very large structures. The Type 1 SEL (Bažant & Xi 1995 Bažant & Li 1995, Bažant & Novák 2000a,b) is then extended as:

$$\sigma_N = \sigma_\infty [(D_b / D)^{rn/m} + rD_b / D]^{1/r} \quad (4)$$

where m = Weibull modulus and n = 1, 2, or 3 for one-, two-, and three-dimensional similarity of fracture. For small sizes, Eq. (4) converges to Eq. (3) for deterministic Type 1 SEL; for large sizes, it approaches Weibull's size effect, i.e., $\sigma_N \sim D^{-n/m}$.

Consequently, the variation of measured fracture energy near the notch tip, generally called the R-curve (or resistance curve), can approximately be

determined from the SEL, using a constant fracture energy G_f:

$$\tilde{G}_f = G_0 D/(D+D_0) \quad (5)$$

$$\tilde{K}_c = K_c\sqrt{D/(D+D_0)} \quad (6)$$

where $G_0 = G_f\, g(\alpha)/g(\alpha_0)$ and $\tilde{K}_c = \sqrt{E\,\tilde{G}}$ (Bažant and Kazemi 1990).

Unlike SEL, BEM attributes the deterministic size effect to the interaction between the FPZ and the structural boundary. Therefore, the energy release due to stress redistribution is disregarded and the term "size" is used to refer to the crack length. By matching the transition between the asymptotic cases 1) of $a \to 0$ and 2) of a and (D - a) both being large, it is postulated that (Hu and Duan 2007, 2008, 2009, Hu and Wittmann 2000):

$$\sigma_n = f_t^{'}/\sqrt{1+a/a_\infty^*} \quad (7)$$

where $a_\infty^* = l_{ch}/1.12^2\,\pi$, $l_{ch} = (K_{IC}/f_t^{'})^2$ = Irwin's characteristic length (Irwin 1958); K_{IC} = critical K_I (fracture toughness); and a is identical to a_0 in SEL. In order to extend Eq. (7) to small ligaments for extremely deep notches (Duan and Hu 2004, Duan et al. 2006, Huan and Duan 2007, 2008, 2009), the nominal strength is redefined as $\sigma_n = \sigma_N/A(\alpha)$. Here $A(\alpha)$ is a geometry constant such that σ_n represent the stress for peak load at the crack tip under the simplifying hypothesis of a linear stress distribution across the ligament, the crack tip stress singularity being ignored; see 1b.

Furthermore, to explain the size dependence of fracture energy measured in tests, a concept of local fracture energy was proposed in BEM. Hu (2002) and Duan et al. (2006) considered the fracture toughness and fracture energy to be variable parameters. Based on Eq. (7), the variable fracture toughness and fracture energy are expressed as

$$K_C = \sqrt{A_1 D/(1+B_1 D)},\ G_f^v = G_F B_1 D/(1+B_1 D) \quad (8)$$

where $G_f^v = K_C^2/E$ (Irwin's relation),

$A_1 = \alpha B(\alpha) K_{IC}^2/a_\infty^*$ and $B_1 = \alpha B(\alpha)/a_\infty^*$

3 INTERPRETATION OF VARIATION OF FRACTURE ENERGY

Rigorously, every physical theory should be formulated in such a way that its constants are actually constant (within the intended scope). If these constants (like $\tilde{G}_f$ and G_f^v) are found to vary, then the theory should be reformulated so that the constant parameters of this variation (here G_f) serve as the new constants. Otherwise, it will destroy the whole theory.

Theoretically, it is unnecessary to use local or variable material properties to interpret the variation of fracture energy observed in tests. What is variable is not the true fracture energy G_F but the *apparent* fracture energy $\tilde{G}_f$ evaluated by classical work-of-fracture method that does not take into account the finiteness of the FPZ caused by material heterogeneity (Bažant 1996, Bažant and Yu 2004).

As shown by Rice in 1968 (Rice 1968), the work integral $G_F = \int_{w=0}^{\infty}\sigma(w)dw$ defining the fracture energy of a cohesive crack is equal to the flux of energy into the FPZ of a propagating crack, given by the J-integral. However, this is true only for quasi-steady crack propagation, during which the stress and strain fields immediately surrounding the FPZ do not change. Near the tip of notch or initial stress-free (fatigued) crack and near the opposite boundary, the propagation is not steady, and the energy flux J required to propagate the crack is smaller than G_F; in detail see Bažant and Yu (2004). When the testing method gives J, or the average J over the ligament (Nakayama 1966, Hillerborg 1985, RILEM 1985), it is not surprising that the fracture energy appears to be variable. So, the idea of a size-dependent fracture energy is an artificial and unnecessary complication. By using a constant G_f, it can also yield the dependence of the R-curve and the apparent fracture energy on the specimen size; see Eqs. (5) and (6).

For accurate measurement of G_F, the unstable crack propagation must happen in a negligible fraction of the specimen size. Therefore the specimen size will be prohibitively large. One has to extrapolate the fracture energy obtained from tests to infinite structure size. This requires a theory that automatically exhibits the size effect, such as the nonlocal softening damage model, the random lattice particle model or, to a limited extent, the cohesive crack model. Jirásek (2003) showed that the variation of apparent fracture energy can be matched by a nonlocal continuum damage model in which the characteristic softening curve is kept fixed. By modifying the tail of cohesive crack model in the unstable cracking zone, Bažant and Yu (2004) also showed that a good agreement could be achieved for Wittmann et al.'s fracture tests (1990). Of course, the nonlocal model is a more general and more fundamental characterization of fracture than the cohesive crack model.

Compared to the total fracture energy G_F, the initial fracture parameter G_f, which is not defined in BEM, is more frequently used in SEL. The advantages of the use of G_f over G_F are that 1) it is size-independent, thus it can be obtained by size effect tests of normal size specimens; 2) it is statistically much less scatter than G_F. Investigation of experimental data reveals that the coefficient of variation of G_F is almost twice as large as that of G_f (Bažant and Becq-Giraudon 2002, Bažant et al. 2002).

4 SIZE EFFECT TEST SUPPLEMENTED BY LOAD-CMOD CURVE

Direct determination of the stress-separation softening function $\sigma(w)$ of cohesive crack model by experiment is next to impossible. Instead, a reverse analysis of test data is generally required to identify the essential aspects of $\sigma(w)$. As is well known, the post-peak response of concrete can be represented realistically if a bilinear softening function $\sigma(w)$ is selected for cohesive crack model. The question now is how to obtain the parameters of this bilinear softening function from the test data, which generally cover only a limited size range and scope.

For the size range used in laboratory, the cohesive stress in the FPZ at peak load still lies completely within the initial steeply descending linear portion of $\sigma(w)$ curve. So, the tail of the softening $\sigma(w)$ cannot play a role in the maximum load. Therefore no information about the tail, which is important to determine the total fracture energy G_F, can be obtained by analyzing the peak load alone, unless extremely large size concrete specimens (i.e., $D > 5$ m) are tested. This limitation applies to all the size effect testing, including both SEL and BEM, in which only the peak load is measured. It means that, to obtain information of the tail, the size effect tests must be supplemented by knowledge of the complete load-deflection curve. Unfortunately, only very limited size effect test data that include the post-peak deflections are available in the literature.

Therefore, new concrete fracture tests on three-point bend beams have been carried out at Northwestern University. In these tests, ready-mixed concrete was procured from Ozinga, Inc., Chicago (470 lb. of Type I cement, 1.20 lb. fly ash, 1680 lb. coarse aggregate of maximum size 9.5 mm, 1540 lb. fine aggregate, and 207 lb. water per cubic yard of concrete were used). The specimens were demolded 1 day after casting and then stored in a standard curing room for 68 days. The notches were cut by a diamond saw 1 month after the casting. Except for a constant width of $b = 40$ mm, the specimens were geometrically scaled; see Fig. 2a. Since larger scatter was expected in the small size range, more small-size than large-size specimens were cast. Tested within 4 days were 10 specimens of $D = 40$ mm, giving the peak loads of 1967, 2007, 2261, 2037, 2008, 2273, 2456, 1922, 2361, and 2185 N; 7 specimens of $D = 93$ mm, giving the peak loads of 3988, 3942, 3683, 3932, 4069, 4249, and 4214 N; and 4 specimens of $D = 215$, giving the peak loads of 6290, 7253, 6965 and 6609 N. The mean Young's modulus $E = 30$ GPa and mean compressive strength $f'_c = 41$ MPa were obtained by testing on 3 standard cylinders of the same concrete.

A relatively low notch-depth ratio α_0=0.15 was selected for the specimens. It led to longer ligaments, which minimized the possible interaction of the crack with the opposite boundary (invoked by BEM). The specimens were tested under crack mouth opening displacement (CMOD) control and

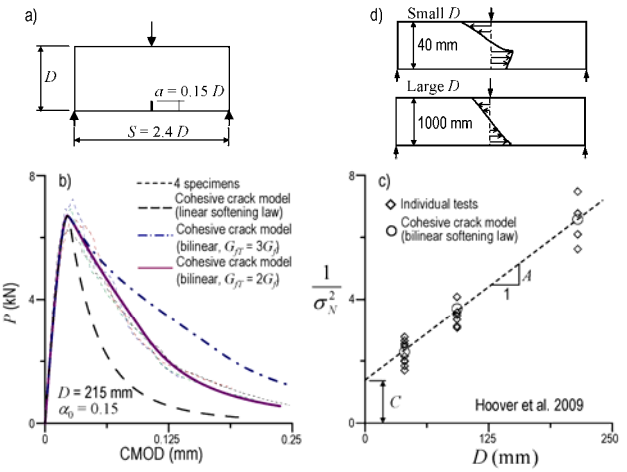

Fig. 2: a) Geometry of tested beams at Northwestern; b) simulation compared to recorded load-CMOD curves; c) simulation compared with recorded peak loads for all sizes; d) normal stress profile in small and large unnotched beams

complete softening curves were recorded for specimens of $D = 215$ mm. As for $D = 40$ and 93 mm, the entire softening curves were not captured because 1) the loading frame was too soft compared to that used for the biggest specimens; and 2) the aggregates traversed by the crack caused in small specimens relatively longer crack jumps.

A finite element code with cohesive crack model was used to fit the measured maximum loads for all sizes. From the measured complete load-CMOD curves, the following $\sigma(w)$ parameters, defined in Fig.1, were identified: $f'_t = 4.80$ MPa, $w_c = 0.08$ mm, $\sigma_1 = 0.2 f'_t = 0.96$ MPa, and $w_1 = 0.0107$ mm. The validity of the selected parameters is documented by the excellent fit of both the complete load-CMOD curves for $D = 215$ mm and the maximum loads P for all the sizes; see Fig. 2b,c.

The bilinear $\sigma(w)$ is fixed by the position of the knee point (w_1, σ_1) and the ratio G_F / G_f. If the tail is dropped (linear cohesive law) or its slope is reduced (G_F increased), the σ_N values for the three sizes can still be matched, but the load-CMOD curve will deviate substantially; see Fig. 2b. The explanation is that the cohesive stresses in the FPZ do not enter the tail within the normal size range of tests; see Fig. 3. If the stress profile along the ligament at peak load is plotted, it can be seen in Fig. 3 that the FPZ is located far away from the boundaries. Note the splitting tensile strength obtained by splitting cylinder test (Brazilian test) may not be a realistic representation of the material tensile strength. The reason is that the splitting tensile strength of Brazilian test also exhibits strong size effect.

5 IDENTIFICATION OF COHESIVE SOFTENING FROM SIZE EFFECT DATA

Compared to the Brazilian tests, the material tensile

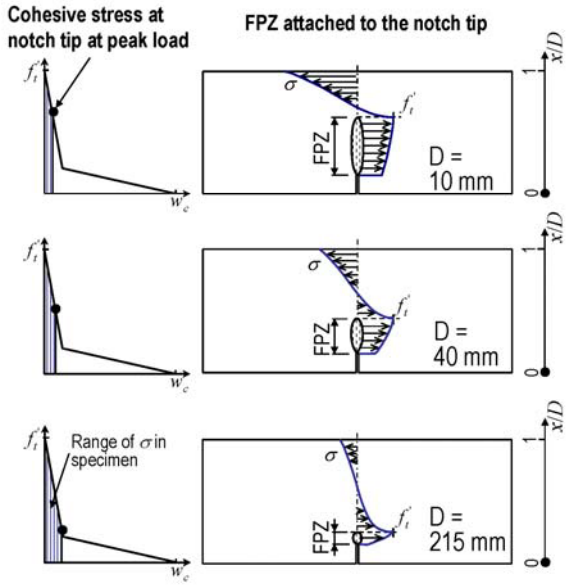

Fig. 3: The FPZ and cohesive stress at notch tip at peak load for beams of different sizes.

strength can be more accurately determined from size effect tests by exploiting Irwin's relation:

$$f_t' = \sqrt{EG_f / l_1}\,, \quad l_1 = c_f / \gamma \tag{9}$$

To obtain f'_t, one must determine parameter γ and decide whether to use the initial fracture energy G_f or the total one, G_F, the latter being more difficult to identify accurately. This problem has been illuminated by cohesive crack simulations of Bažant et al. (2002) and especially Cusatis and Schauffert (2009), who showed that $\gamma = 0.44$ for the linear softening (and $\gamma = 2.31$ for bilinear softening and G_F replacing G_f). However, these values are only approached for $D \to \infty$. For decreasing D, the cohesive crack results deviate from the Type 2 SEL linear regression line appreciably. Therefore, correction must be undertaken.

If the total fracture energy G_F of bilinear softening is considered, the regression line will approach its asymptote closely only for specimen sizes far beyond the laboratory range, precisely for $D_l > 10$ where D_l is dimensionless shape-independent size,

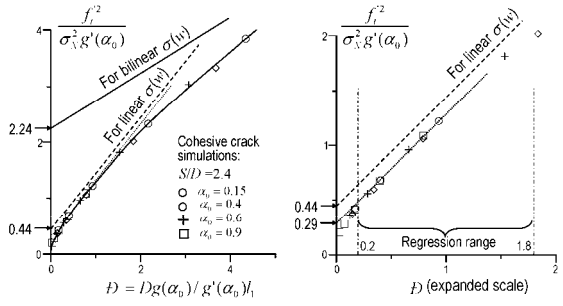

Fig. 4: Dimensionless plots of size effect simulations by cohesive crack model and their asymptotes.

equal to $Dg_0 / l_{ch}\, g'_0$ ($l_{ch} = EG_F / f_t'^2$). If the tail is dropped and only the initial softening slope is considered, the asymptote will become steeper and will be approached closely for sizes an order of magnitude smaller. Cusatis and Schauffert (2009) find that the asymptotic slope corresponding to G_f is best obtained by tests within the range $0.2 < D_l < 0.7$ for bilinear softening.

However, Cusatis and Schauffert obtained this result by positing the knee point of bilinear softening curve at $\sigma_1 = 0.25 f_t'$. They did not investigate the effect of σ_1 on the optimal size range for G_f. By keeping G_f, G_F and f'_t constant while moving σ_1 up and down in the bilinear softening curve, it is found in this study that the optimal size range ($0.2 < D_l < 0.7$) will not change significantly for typical geometry used in 3-point bend tests when $\sigma_1 \le 0.25 f_t'$. When the knee point is higher than $0.25 f'_t$, the optimal D_l will shift to smaller sizes. The reason is that, for a higher σ_1, the cohesive strength in the FPZ enters the tail for smaller sizes. Fortunately, for normal concrete, the knee point is usually lower than $0.25 f'_t$ (CEB 1991), therefore this optimal size range can generally be used in data analysis. Since this optimal size range depends mainly on G_f, it is better to change the definition of the dimensionless shape-independent size to $Đ = Dg_0 / l_1\, g'_0$ ($l_1 = EG_f / f_t'^2$). Then the optimal size range will be $0.4 < Đ < 1.4$ and it will be almost independent of the ratio G_F/G_f.

It should be pointed out that this optimal size range, obtained by cohesive crack model only, may be statistically insufficient if the inevitable randomness of test is considered. To minimize the effect of random scatter on the data fitting, it is statistically preferable that the size range be at least 1:8 (Bažant and Planas 1998). Therefore, it is desirable to extend this size range at least to $Đ$ in (0.2, 1.8).

To investigate the possibility of extending the testing range, the program for the cohesive crack model was run for specimens of $\alpha_0 = 0.15$, 0.4 and 0.6, span-to-depth ratio $S/D = 2.4$, 4, and 8, and size D from 40 to 1000 mm. This covers all the shapes typically used in three-point bend tests. Various linear size effect regressions for various α and S/D were conducted. The parameters obtained are listed in Table 1.

As stated by Cusatis and Schauffert (2009), if $\sigma(w)$ is linear, the asymptote gives $\gamma = 0.44$. But to achieve this asymptote requires an unacceptably large size ($Đ > 10$). Fortunately, it turns out that testing extremely large specimens is not necessary when a bilinear $\sigma(w)$ is used. By virtue of the transition to the second asymptote corresponding to the $\sigma(w)$ tail, it luckily happens that, in the normal size range ($0.4 < Đ < 1.4$), the curve in Fig.4 computed from the cohesive crack model is almost parallel to the asymptote for the linear softening that gives G_f. The downward shift from this asymptote actually represents the intermediate asymptote in the sense of

Table 1: Slope and intercept of regression line.

	S/D = 2.4		S/D = 4		S/D = 8	
$Đ$	0.4-1.4	0.2-1.8	0.4-1.4	0.2-1.8	0.4-1.4	0.2-1.8
Slope	0.99	0.99	1.02	1.01	1.04	1.03
γ	0.286	0.276	0.290	0.281	0.292	0.286

Barenblatt (1996, 2003). The values for γ other than 0.44 are listed in Table 1 according to the shape and size range. It is for this reason that the SEL regression of σ_N data from the cohesive crack model yields excellent agreement for G_f, as well as l_1 and f'_t.

If the size range of specimens is extended to $Đ$ in (0.2, 1.8), which helps to minimize the scatter of the regression slope of test data, the results of regression for G_f are almost same. But for c_f and f'_t it is then better to reduce γ from 0.29 to 0.28, in order to compensate for the small downward shift of the regression line due to the curvature of the plot outside the interval (0.4, 1.4). A proper adjustment of γ would permit even broader size ranges, such as 1:16.

For bilinear softening, the size range for acceptable estimation of G_f is $0.2 < Đ < 1.8$ (after extension), which most of the laboratory specimens fall in. Therefore, for most size effect tests, the G_f obtained from regression according to SEL is in good agreement with the cohesive crack model, while the f'_t is much larger. This is due to the c_f obtained is far less than the real c_f. Fortunately, by using the correction listed in Table 1, an accurate estimate of f_t' is obtainable.

After G_f and f_t' are determined by size effect test data, G_F and the knee position can be identified by matching the measured load-CMOD curves.

6 QUESTIONALBLE ASPECTS IN BEM

Besides the misleading interpretation of the variation of the apparent fracture energy, a careful study shows there are other fundamental flaws in BEM.

1. Incorrect hypothesis about the size effect mechanism and FPZ/boundary interactions. In BEM, it is asserted (Hu and Duan 2008) that the size-dependence of quasibrittle fracture transition is actually due to the interaction of FPZ with the nearest structure boundary and the SEL is only a special case for quasibrittle fracture controlled by the FPZ and boundary interaction. This assertion is untrue. When the ligament length (D-a) and the crack length a are both much larger than the FPZ length, one obtains the strongest size effect possible – the size effect of the LEFM. Yet in that case there is no interaction with the boundary because the FPZ is surrounded by the LEFM near-tip stress field, which is independent of the boundary geometry.

2. Disregard of energy balance condition. If σ_N and the structure geometry are kept constant, the calculated rate of energy release from the structure increases with structure size D. To ensure that it remain equal to the rate of energy dissipation in the FPZ of a crack, σ_N must decrease with increasing D (Bažant 1984, 2004, 2005). The derivation of BEM ignores this undeniable source of size effect.

3. Ambiguity of stress profile definition and of σ_n. The definition of σ_n and of the stress profile across the ligament becomes ambiguous when extended beyond a few basic types of Mode I fracture specimens. When applied to mixed mode or complex geometries, it is non-unique and dubious; see Fig. 5. On the other hand, function $g(\alpha)$ on which the SEL is based can be unambiguously calculated for all these cases.

4. Incorrectness of linear stress profile in asymptotic cases. When the size D is small or the ligament is small, a linear stress profile proposed in BEM is not realistic. Instead, a rectangular stress profile must be asymptotically approached.

5. Problematic definition of a_e. In BEM, the asymptotic cases of crack initiation from the surface and of vanishing ligament (extremely deep notch) are amalgamated by the hypothesis of an equivalent crack length a_e (Duan et al. 2006). However, this hypothesis is based on an unjustified assumption of a linear stress profile.

6. No mathematical basis for asymptotic matching. Unlike the rigorous mathematic derivation in SEL to match, up to the second-order, the asymptotic properties, the procedure to set up Eq. (7) is intuitive. The mathematic basis of the selection of Eq. (7) is not documented.

7. Limited range and scope of application. By taking advantage of selecting the same transition as SEL between the asymptotic cases, BEM generates realistic G_f values (in BEM it is treated as total fracture energy) for normal notch ratios and large enough structures, provided they fail in a simple fracture mode. However, due to its unrealistic hypotheses, the BEM gives poor predictions for small sizes, shallow notches and short ligaments, and also for material tensile strength f'_t (peak cohesive stress).

8. Unrealistic hypothesis of proportionality of flaw size to structure size. To extend Eq. (7) to the extreme case $\alpha = 0$ (Type 1 in SEL), BEM assumes that the size of the largest flaw, which is treated as

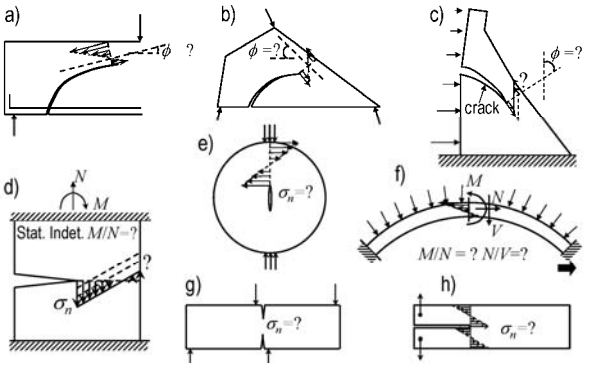

Fig. 5: Examples of specimens and structures for which BEM cannot be used but SEL can.

the pre-existing crack, is proportional to the structure size. However, the flaw size distribution is strictly a material property and thus cannot be a function of the structure size. Otherwise, Freudenthal-type (1968) analysis relating the flaw size distribution to the statistical size effect in structures would yield a Weibull statistical distribution in which the shape and scale parameters would be size dependent. Yet they are not.

9. Incorrect large-size asymptote for failures at crack initiation. In Eq. (7), same large-size asymptotic slope –1/2 (LEFM) is given for both unnotched and notched specimens. This differs from the results obtained by tests and by cohesive crack simulations.

10. Absence of a statistical part of size effect at crack initiation. In Eq. (4) of SEL, statistical size effect is amalgamated with the deterministic size effect. However, in BEM, this part is missing.

11. Incorrect material strength identified by BEM. In BEM, σ_n is directly related to f'_t by the linear stress profile, and the tensile strength can thus be obtained directly by linear regression of test data. However the resulting tensile strength severely disagrees with the cohesive crack simulations.

7 COMPARING SEL AND BEM BY EXTENDING TESTS THROUGH COHESIVE CRACK MODEL

To compare SEL and BEM thoroughly, simulation results of beams of $S/D = 2.4$ and of variable notch to depth ratios, which include a smooth surface ($\alpha_0 = 0$) and an extremely deep notch ($\alpha_0 = 0.9$), are investigated. The cohesive softening curve obtained from the tests at Northwestern is used in all the simulations.

Unnotched beams of the same shape as the tested specimens are first numerically simulated. Here the largest size of beam is extended up to $D = 1$ m. The error of BEM, which is obscured by an insufficient size range and inevitable test randomness in data fitting, is now strikingly exposed. If BEM were true, a linear regression of the data should conform to a linear plot of $1 / \sigma^2_N$ versus D. But Fig. 6 documents a very poor fit (solid line), with $\rho^2 = 0.67$ (ρ = correlation coefficient). By contrast, the SEL Type 1 gives an excellent fit, with $\rho^2 = 0.99$ (dashed curve). The simulated size effect curves for notches ranging from $\alpha_0 = 0$ to $\alpha_0 = 0.9$ and D up to 1 m are shown in the logarithmic scale in Fig. 6. It can be clearly seen that the size effect trend of unnotched beams closely approaches a horizontal asymptote, agreeing with the deterministic Type 1 SEL but contradicting the slope –1/2 dictated by BEM. In Fig.2d the stress profiles at peak loads for notchless beams of $D = 40$ and 1000 mm are compared. For size $D =$ 1000 mm, the stress profile is almost linear, which implies that the deterministic size effect must disappear for larger sizes. Obviously, the BEM is unrealistic.

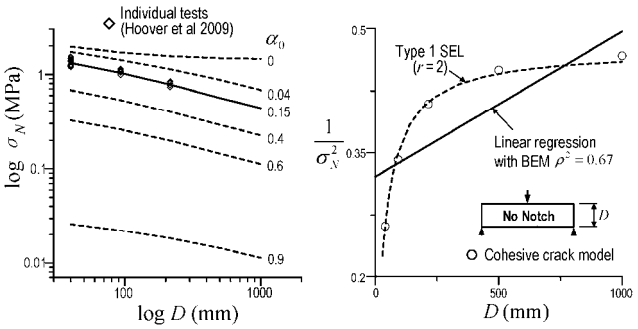

Fig. 6: Left: Nominal strength values obtained by cohesive crack model for various α_0; right: linear regression according to BEM for no notch ($\alpha_0 = 0$) of computer results by cohesive crack model.

The parameters of SEL (Type 2) and BEM, obtained by linear regression, are listed in Table 2 and compared in Fig. 7. But no SEL parameters are listed for $\alpha_0 < 0.04$ because SEL is not applicable for such shallow notches. For notchless beams, an imaginary notch $\alpha_0 = 0.02$, based on the ratio of maximum aggregate size to $D = 500$ mm, is assumed for BEM calculations. From Table 1, it can be seen that $\gamma = 0.286$ for D in (0.4, 1.4) and $S/D = 2.4$. Computer simulations show that $\gamma = 0.29$ gives good results (much better than BEM) for all three-point bend beams with typical S/D (2.4 to 8) and medium notch depths ($0.15 < \alpha_0 < 0.6$); see Table 1.

As seen in Table 2, the scatter of f'_t values over the full range of α_0 is significant for the BEM, even though it claims to cover all notch depths. The FPZ in Fig. 3, which is far away from the boundaries, further invalidates the BEM hypothesis about the interaction between FPZ and the boundary. On the other hand, the SEL based testing of G_f, c_f and f'_t gives acceptable results for $0.15 < \alpha_0 < 0.6$, which is in the recommended testing range. For $\alpha_0 = 0.04$ and 0.9, which are not within the recommended range of SEL testing, the regression results deviate from cohesive crack model considerably.

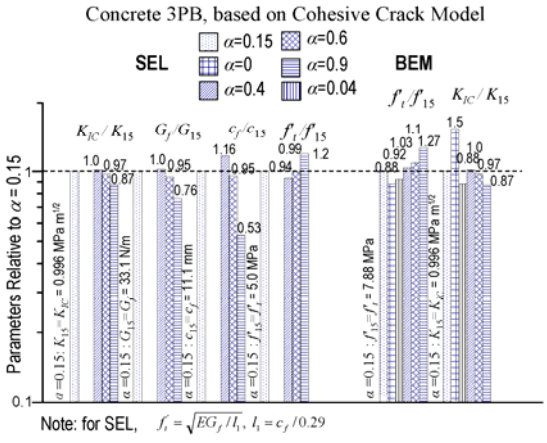

Fig. 7: Comparison of the results of SEL and BEM with cohesive crack model.

One advantage over SEL claimed by BEM is that BEM obtains K_{IC} and f'_t by testing various α_0 for one size only. So, not surprisingly, the scatter seen in Table 2 is much larger than it is for the SEL. This is a serious deficiency of the BEM testing method. Contrary to the opinion of Hu and Duan, testing at different sizes cannot be avoided, as already concluded in Tang et al. (1996). The reason is that a sufficient range of brittleness numbers can never be attained by merely varying the notch depth at constant size (Tang et al. 1996). The f'_t values obtained by BEM severely disagree with the cohesive crack model for every notch depth (Table 2). For the extre mes $\alpha_0 = 0$ and 0.9, they are 6.96 MPa and 10.0 MPa, although the essential hypothesis of the BEM is that extremely shallow and extremely deep notches should have the same asymptote, with $\sigma_n \rightarrow f'_t$. The BEM generally overestimates f'_t by about 70%. This observation also strengthens the objection that the small-size asymptote of the BEM based on a linear stress profile across the ligament is fundamentally unjustifiable. Thus it must be concluded that while the BEM testing method does directly give the tensile strength, its values are quite unrealistic.

To generate a constant tensile strength, the BEM would have to use test specimen sizes falling in the optimal range $0.2 < D < 1.8$, which cannot be achieved by varying the crack length only. When the size is within the optimal range, the BEM will generate a consistent $f'_t \approx 8.2$ MPa for notched beams. However this value is very different from the cohesive tensile strength identified by matching the load-CMOD curves and the peak loads of all specimens. Asymptotically for vanishing sizes, the cohesive crack is equivalent to a plastic glue with yield strength f'_t (Bažant et al. 2002). Hence, for a three-point bend beam, one obtains $B = 2D(1-\alpha_0)^2/S$. Using cohesive crack model to simulate an extremely small specimen to obtain the σ_N, i.e., $\sigma_N = 2.7$ MPa for $D = 0.1$ mm and $\alpha_0 = 0.15$, one can calculate $f'_t = 4.5$ MPa, close to the cohesive tensile strength.

8 UNIQUENESS OF COHESIVE SOFTENING OBTAINED BY WORK-OF-FRACTURE TEST

A problem related to the comparison of SEL and BEM is the uniqueness of the bilinear softening curve identified by matching the measured load-CMOD curve. As recently found, it is not sufficient to determine the tensile strength f'_t and initial fracture energy G_f by fitting the load-CMOD curve for one size only. Fig. 8a shows four load-CMOD curves of a notched beam 215 mm deep obtained by four different sets of $\sigma(w)$ parameters with f'_t ranging from 4.4 to 8.2 MPa and G_f from 21 to 35 N/m while G_F is fixed at 64 N/m. Although the aforementioned parameters of cohesive softening function $\sigma(w)$ vary appreciably (G_f by 68%), the differences among the resulting load-CMOD curves are negligible compared to the random scatter in testing.

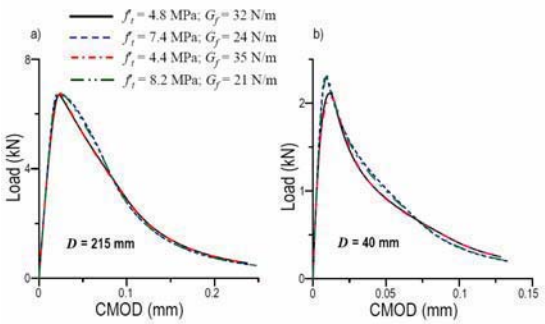

Fig. 8: Load-CMOD curves obtained by 4 different bilinear softening curves.

Therefore, testing the size effect is indispensable for a unique identification of the bilinear softening curve of cohesive crack model, and especially the determination of the initial fracture energy G_f. Fig. 8b shows the same four different cohesive softening curves are applied to a small specimen of $D = 40$ mm. It can now be clearly seen that, for this second size, the obtained peak loads and the load-CMOD curves are quite different. The peak load predicted by parameter set of $f'_t = 8.2$ and $G_f = 21$ N/m is about 13% higher than that of parameter set of $f'_t = 4.4$ MPa and $G_f = 35$ N/m. And this is for sizes in the ratio of only 5.3 : 1. If the size ratio is increased, the differences will become larger.

Therefore, in order to identify the bilinear cohesive curve, the work of fracture test must be supplemented by size effect test, and the size range must be sufficiently large (probably ≥ 1:8). Only the cohesive softening curve that yields a close match of both the load-deflection curve and the peak loads over a sufficient size range can be treated as the realistic representation of the fracture parameters.

9 CONCLUDING REMARKS

The size effect is a salient feature of quasibrittle

Table 2: Material parameters obtained by SEL and BEM.

α_0	Cohesive crack Model				Size Effect Law				Boundary Effect Model		
	K_{IC}	G_f	f'_t	G_F	K_{IC}	G_f	f'_t	c_f	$A(\alpha)$	K_{IC}	f'_t
0	0.98	32	4.8	64	-	-	-	-	0.96	1.53	6.96
0.04	"	"	"	"	-	-	-	-	0.92	0.88	7.28
0.15	"	"	"	"	0.996	33.1	5.0	11.1	0.72	0.996	7.88
0.40	"	"	"	"	1.01	33.8	4.68	12.96	0.36	1.01	8.15
0.60	"	"	"	"	0.969	31.3	4.98	10.58	0.16	0.969	8.58
0.90	"	"	"	"	0.869	25.2	5.98	5.91	0.01	0.869	9.99

fracture and inseparable from experimental identification on its characteristics. Efforts to identify the quasibrittle fracture parameters by measuring the load-CMOD curve at one size are futile. So are the efforts to replace the tests of size effect on the nominal strength by strength tests at different crack lengths. The effect of the proximity of the boundary is not the cause of size effect and does not imply a variation of the total and initial fracture energies as parameters of a properly defined softening cohesive stress-separation law. These are apparent phenomena explicable as consequences of this law.

ACKNOWLEDGMENT

Support by the U.S. Department of Transportation through Grant 20778 from the Infrastructure Technology Institute of Northwestern University is gratefully acknowledged.

REFERENCES

Barenblatt, G.I. 1959. The formation of equilibrium cracks during brittle fracture, general ideas and hypotheses, axially symmetric cracks, Prikl. Mat. Mech., 23(3), 434-444.

Barenblatt, G.I. 1996. Scaling, Selfsimilarity and Intermediate Asymptotics. Cambridge Univ. Press (Cambridge, UK).

Barenblatt, G.I. 2003. Scaling. Cambridge Univ. Press (Cambridge, UK).

Bažant, Z.P. 1984. Size effect in blunt fracture: Concrete, rock, metal. J. Engrg. Mech., ASCE, 110(4), 518-535.

Bažant, Z.P. 1996. Analysis of work-of-fracture method for measuring fracture energy of concrete, J. of Engrg. Mechanics ASCE 122 (2), 138-144.

Bažant, Z.P. 1997. Scaling of quasibrittle fracture: Asymptotic analysis, Int. J. of Fracture 83 (1), 19-40.

Bažant, Z.P. 2004. Scaling theory of quaisbrittle structural failure, Proc. Nat'l. Acad. Sci., USA 101 (37), 13397-13399.

Bažant, Z.P. 2005. Scaling of Structural Strength, 2nd Ed., Elsevier, London.

Bažant, Z.P., and Becq-Giraudon, E. 2002. Statistical prediction of fracture parameters of concrete and implication for choice of testing standard, Cement and Concrete Research 32(4), 529-556.

Bažant, Z.P., and Kazemi, M.T. 1990. Determination of fracture energy, process zone length and brittleness number from size effect, with application to rock and concrete, Int. J. of Fracture, 44, 111-131.

Bažant, Z.P., and Li, Z. 1995. Modulus of rupture: size effect due to fracture initiation in boundary layer, J. Struct. Engrg. ASCE, 121 (4), 739-746.

Bažant, Z.P., and Novák, D. 2000a. Probabilistic nonlocal theory for quasibrittle fracture initiation and size effect. I. Theory, J. of Engrg. Mech. ASCE 126 (2), 166-174.

Bažant, Z.P., and Novák, D. 2000b. Probabilistic nonlocal theory for quasibrittle fracture initiation and size effect. II. Application, J. of Engrg. Mech. ASCE 126 (2), 175-185.

Bažant, Z.P. and Planas, J. 1998. Fracture and Size Effect in Concrete and Other Quasibrittle Materials, CRC Press.

Bažant, Z.P. and Xi, Y. 1991. Probabilistic nonlocal theory for quasibrittle failure initiation and size effect. II. Application. J. Engrg. Mech. 126(2), 175-185.

Bažant, Z.P., and Yu, Q. 2004. Size effect in concrete specimens and structures: New problems and progress, Fracture Mechanics of Concrete Structures (Proc., FraMCoS-5, 5th Int. Conf. on Fracture Mech. of Concrete and Concr. Structures, Vail, Colo.), Vol. 1, V.C. Li, K.Y. Leung, Willam, K.J., and Billington, S.L., eds., IA-FraMCoS, 153--162; republished in Acta Polytechnica (Prague) 44 (5-6), 7-15, 2004.

Bažant, Z.P., Yu, Q., and Zi, G. 2002. Choice of standard fracture test for concrete and its statistical evaluation, International Journal of Fracture, 111, 303-337.

CEB. 1991. CEB-FIP model code 1990, final draft. Bulletin d'Information du Comité Euro-International du Béton, 203-205.

Cusatis, G., and Schauffert, E.A. 2009. Cohesive crack analysis of size effect, Engrg. Fracture Mechanics 76, in press.

Duan, K. and Hu, X.Z. 2004. Specimen boundary induced size effect on quasi-brittle fracture, Strength, Fracture and Complexity, 2(2), 47-68.

Duan, K., Hu, X.Z., and Wittmann, F.H. 2006. Scaling of quasi-brittle fracture: Boundary and size effect, Mech. Mater. 8, 128-141.

Freudenthal, A. M. 1968. Statistical approach to brittle fracture, In: Liebowitz, H. (Ed.), Fracture: An Advanced Treatises, vol. 2, Academic Press, New York, 591-619.

Hillerborg, A. 1985. The theoretical basis of a method to determine the fracture energy GF of concrete, Materials and Structures, 18, 291-296.

Hillerborg, A., Modéer, M., and Petersson, P.E. 1976. Analysis of crack formation and crack growth in concrete by means of fracture mechanics and finite elements, Cem. Concr. Res. 6, 773-782.

Hu, X.Z. 2002. An asymptotic approach to size effect on fracture toughness and fracture energy of composites, Engrg. Frac. Mech. 69, 555-564.

Hu, X.Z. and Duan, K. 2007. Size effect: Influence of proximity of fracture process zone to specimen boundary, Engrg. Frac. Mech. 74, 1093-1100.

Hu, X.Z. and Duan, K. 2008. Size effect and quasi-brittle fracture: the role of FPZ, Int. J. Frac. 154, 3-14.

Hu, X.Z. and Duan, K. 2009. Mechanism behind the size effect phenomenon, Manuscript submitted to J. of Engrg. Mech.

Hu, X.Z. and Wittmann, F.H. 1992. Fractrue energy and fracture process zone, Materials and Structures 25, 319-326.

Hu, X.Z. and Wittmann, F.H. 2000. Size effect on toughness induced by crack close to free surface, Engrg. Frac. Mech. 65, 209-221.

Irwin, G.R. 1958. Fracture. In Handbuch der Physik, Vol. 6, Flügge, ed., Springer-Verlag, Berlin, 551-590.

Jirásek, M. 2003. Keynote lecture presented at EURO-C, St. Johann in Pongau, Austria.

Nakayama, J. 1965. Direct measurement of fracture energies of brittle heterogeneous material, J. of the Am. Ceramic Society 48 (11), pp. 583-587.

Nallathambi, P., Karihaloo, B.L., and Heaton, B.S. 1984. Effect of specimen and crack size, water cement ratio and coarse aggregate texture upon fracture toughness of concrete. Mag. Concrete Res. 36 (129), 227-236.

Petersson, P.E. 1981. Crack growth and development of fracture zone in plain concrete and similar materials, Report No. TVBM-1006, Division of Building Materials, Lund Institute of Technology, Lund, Sweden.

Rice, J.R. 1968. Mathematical analysis in the mechanics of fracture - an advanced treatise Vol.2, (ed. Liebowitz, H.), Academic Press, New York, 191-308.

RILEM. 1985. Determination of the fracture energy of mortar and concrete by means of three-point bend tests on notched beams, RILEM Recommendation TC 50-FMC Materials and Structures 18, 285-290.

Tang, T., Bažant, Z.P., Yang, S., and Zollinger, D. 1996. Variable-notch one-size test method for fracture energy and process zone length, Engineering Fracture Mechanics, 55 (3), 383-404.

Wittmann, F.H., Mihashi, H., and Nomura, N. 1990. Size effect on fracture energy of concrete, Engrg. Fracture Mech. 35, 107-115.

Yu, Q., Le, J.-L., Hoover, G. and Bažant, Z.P. 2010. Problems with Hu-Duan Boundary effect model and its comparison to size-shape effect law for quasibrittle fracture, J. of Engrg. Mech. ASCE 125 (1), in press.